

Accepted Manuscript

The tribological properties of short range ordered W-B-C protective coatings prepared by pulsed magnetron sputtering

S. Debnárová, P. Souček, P. Vašina, L. Zábranský, V. Buršíková, S. Mirzaei, Y.T. Pei



PII: S0257-8972(18)31123-X
DOI: doi:[10.1016/j.surfcoat.2018.10.026](https://doi.org/10.1016/j.surfcoat.2018.10.026)
Reference: SCT 23889

To appear in: *Surface & Coatings Technology*

Received date: 16 August 2018
Revised date: 8 October 2018
Accepted date: 9 October 2018

Please cite this article as: S. Debnárová, P. Souček, P. Vašina, L. Zábranský, V. Buršíková, S. Mirzaei, Y.T. Pei , The tribological properties of short range ordered W-B-C protective coatings prepared by pulsed magnetron sputtering. Sct (2018), doi:[10.1016/j.surfcoat.2018.10.026](https://doi.org/10.1016/j.surfcoat.2018.10.026)

This is a PDF file of an unedited manuscript that has been accepted for publication. As a service to our customers we are providing this early version of the manuscript. The manuscript will undergo copyediting, typesetting, and review of the resulting proof before it is published in its final form. Please note that during the production process errors may be discovered which could affect the content, and all legal disclaimers that apply to the journal pertain.

The tribological properties of short range ordered W-B-C protective coatings prepared by pulsed magnetron sputtering

S. Debnárová ^{1*}, P. Souček ¹, P. Vašina ¹, L. Zábranský ¹, V. Buršíková ¹, S. Mirzaei¹, Y.T. Pei ²

¹ Department of Physical Electronics, Masaryk University, Kotlářská 2, CZ-61137 Brno, Czech Republic

² Department of Advanced Production Engineering, Engineering and Technology Institute Groningen, Faculty of Science and Engineering, University of Groningen, Nijenborgh 4, 9747AG Groningen, The Netherlands

* Corresponding author: S. Debnárová, email: debnarova@mail.muni.cz, telephone: +420 549 49

Abstract (max. 300 words)

In this study mid-frequency pulsed-DC magnetron sputtering was used to deposit W-B-C coatings. The effect of coating composition and the deposition parameters on the structure, mechanical and tribological properties of the coatings was investigated. The broad diffraction peaks in the X-ray diffractogram indicated the amorphous to nanocrystalline nature of the coatings. The hardness of the coatings ranged from 22.6 to 26.2 GPa. The coatings prepared at the elevated temperature of 500°C exhibited greater hardness compared to the coatings prepared at the ambient temperature. The amount of W in the coatings was the main parameter influencing the friction coefficient with a higher W content leading to a higher friction coefficient. The coatings prepared at 500 °C showed lower wear in tribological measurements due to their higher hardness compared to the coatings prepared at ambient temperature. The friction coefficient decreased as the testing temperature increased beyond 500 °C. XRD analyses after the high temperature tests have shown that this decrease was due to the formation of W-O Magnéli phases, which acted as a solid-state lubricant.

Keywords: W-B-C; thin films; magnetron sputtering; protective coatings; tribological properties

1 Introduction

The protection of tools for metal machining is one of the most widely used applications for protective coatings. The hard ceramic based coatings used nowadays, such as TiN, TiAlN and c-BN, are examples of typical protective industrial coatings [1-5]. Although they exhibit high hardness and stiffness, they also exhibit brittle behaviour facilitating the propagation of cracks in the coating once a crack is formed. This can lead to premature failure of the coating and the tool itself. A solution for this problem would be the use of protective coatings that are simultaneously hard, stiff and moderately ductile.

Two criteria are commonly used to determine the deformation behaviour of materials. Brittle materials generally exhibit a ratio of bulk modulus (B) to shear modulus (G) smaller than 1.75 [4, 6]. A negative Cauchy pressure, calculated as the difference of two elastic constants ($C_{12} - C_{44}$), is another indication of brittle behaviour [4, 6]. Figure 1 shows the Cauchy pressure and the B/G ratio of TiN [7], TiB₂ [8] and c-BN [9] - commonly used protective coatings. They exclusively fall into the brittle region with a B/G ratio < 1.75 and a negative Cauchy pressure shaded in red. Recently, a crystalline system consisting of transition metal, boron and carbon in a X₂BC stoichiometry was predicted to exhibit high hardness and moderate ductility by ab initio calculations [6]. W₂BC was predicted to exhibit the highest Cauchy pressure and the highest B/G ratio of the studied systems [6], falling into the ductile region as plotted in Fig. 1 for comparison. In addition to the enhanced ductility the X₂BC coatings are also predicted to exhibit the bulk modulus and thus stiffness comparable to, or even exceeding the commonly used hard protective coatings.

The experimental focus in the studies of the X₂BC materials has so far been centred on another material of this group, namely Mo₂BC [10, 11, 12, 13]. Crystalline Mo₂BC coatings were prepared by DC magnetron sputtering at a temperature of ≥ 800 °C [10]. In order to lower the required substrate temperature, high power pulses were used leading to a reduction

in the temperature needed for Mo₂BC crystallization to ~ 400 °C [11]. Tensile tests were performed to study the damage behaviour of the Mo₂BC coatings that exhibited a significantly higher cracking resistance compared to the benchmark TiAlN coatings [13].

The unusual combination of high hardness and moderate ductility predicted for crystalline X₂BC material is due to the structure of the unit cell [6]. The unit cell consists of alternating regions of high electron density and strong covalent bonds (W-B, W-C) and regions of low electron density and weaker metallic bonds (W-W). These regions form a naturally nanolaminated structure, within which the layers of strong covalent bonds are responsible for the high toughness and hardness of the material, while the material is able to deform plastically along the layers of weaker metallic bonds allowing for simultaneously ductile behaviour.

However, high hardness, enhanced ductility and fracture resistance are not the only parameters influencing the performance of coated tools during real-life applications. The protective coatings should also display suitable tribological properties such as low friction coefficient (CoF) and low wear to limit the damage to the coating caused by abrasion or surface fatigue e.g. during high speed or dry cutting [14]. The commonly used ceramic based protective coatings exhibit high hardness (~ 30 GPa) but also a high friction coefficient. For example, the values of the CoF range from 0.7 to 1.2 for TiN [15, 16] and from 0.75 to 0.85 for TiAlN [17, 18] making these materials unsuitable for the most demanding applications. There are no reports on the tribological properties of coatings simultaneously composed of W, B and C available in the literature. The friction coefficient of binary or ternary coatings containing W, B and/or C can range from 0.15 for B₄C [19] to 0.82 for boron doped W coatings [20].

The present work explores the mechanical, structural and primarily tribological properties of W-B-C coatings with differing structures and composition. Six W-B-C coatings with 3

different compositions each at 2 different deposition temperatures were deposited and analysed using a variety of methods. The influence of coating composition and deposition temperature on the structure, mechanical properties, friction coefficient and wear rate was investigated in detail. Tribological tests at elevated temperatures were conducted to study the tribological properties of the coating in applications without cooling or lubrication, where high temperatures of the workpiece are common.

2 Experimental setup

A Vinci Technologies PVD 50S magnetron sputtering rig was used for depositions. W, B₄C and C targets with purities of 99.95%, 99.5% and 99.999% respectively were sputtered. The targets were circular with a diameter of 3 inches (~ 7.6 cm) located in the sputter-down configuration and were aimed onto a central substrate holder at a distance of 18 cm. The W and B₄C targets were each powered by a Power Mag Technologies Maxim 1000 DC generator, while the C target was powered by an Advanced Energy Pinnacle plus mid-frequency pulsed DC generator, which was set to the frequency of 350 kHz at 65% duty cycle. Pulsed-DC plasma excitation instead of simple DC was used to enhance the ion bombardment and the energy flux to the growing coating [21]. Mid-frequency pulsed-DC leads mainly to the ionisation of background gas and not the sputtered species. Therefore, the target with the greatest mean power applied to it (C) was set up to be pulsed-DC driven. The coatings were deposited on a silicon (100) wafer for SEM cross-section imaging and analyses of the chemical composition, cemented tungsten carbide for XRD analyses and nanoindentation tests and high-speed steel substrates for tribological measurements.

The substrates were first ultrasonically cleaned in a degreasing agent before the deposition, then they were placed into the chamber and further cleaned by ion bombardment in a RF (13.56 MHz) argon plasma for 20 minutes. The pressure was set to 0.3 Pa with Ar flow of 5

sccm, and the bias voltage on the substrate was -200 V during the cleaning process. During deposition, the pressure was always kept at 0.2 Pa and the substrate holder was rotating at 5 rpm. Three sets of coatings were deposited with different sputtering powers applied to the individual targets. Each set of the coatings included two coatings deposited at two different temperatures (ambient temperature $\sim 50^{\circ}\text{C}$ and 500°C). The deposition conditions of the coatings are summarized in Table I. The duration of the deposition was always 7 hours and the thickness of the coatings was 1.75 - 2.25 μm .

A Tescan MIRA3 scanning electron microscope was used for the SEM imaging. An Oxford Instruments X-MAX^N 50 EDX detector connected to the SEM chamber was used to measure the chemical composition of the coatings. The quantification of the elemental composition was made using an internal standards library supplied by Oxford Instruments within AZtec Software. Since evaluating the boron and carbon content of these coatings using EDX can be difficult, a calibration using Rutherford backscattering spectroscopy for several samples was conducted. Rigaku SmartLab Type F in the grazing angle of incidence configuration (GIXRD) was used to analyse the crystalline structure. The angle of incidence of the copper $K\alpha$ X-ray ($\lambda = 1.54056 \text{ \AA}$) source was set to 0.5° . A Hysitron Triboindenter TI950 with a Berkovich tip was used to evaluate the mechanical properties. A quasistatic test with 20 segments of increasing load in the range from 50 μN to 11 mN was conducted. The hardness and effective elastic modulus values were determined at indentation depths where the substrate influence was negligible. The standard procedure proposed by Oliver and Pharr [22] was used.

A CSM high temperature ball on disc tribometer was used to evaluate the tribological properties of the coatings. The sliding counterpart was a ball with a diameter of 6 mm made from ceramic Si_3N_4 with a hardness of 17.7 GPa. The measurements were conducted in air with a constant humidity of 35%. All coatings were analysed at a constant rotation speed of 10 cm/s. The length of the track was 200 m. Two different loads were used, namely 1 N and 5

N. The measurements were conducted at ambient temperature and elevated temperatures of 300, 500 and 600°C. The wear rate was evaluated using an Olympus OLS 4000 laser confocal microscope. A 3D image of the wear track was taken and the wear volume was calculated using Olympus control software supplied with the confocal microscope.

3 Results and discussion

The W-B-C coatings investigated in this work are summarised in Table I. Three pairs of coatings labelled 1-3 were deposited with different sputtering powers that resulted in different composition. Each coating pair consisted of one coating deposited at ambient temperature (AT) and one deposited at 500°C. Coating 1 had the lowest content of W, coating 2 had a composition close to the W_2BC stoichiometry and coating 3 had the highest content of W. Figure 2 shows the composition of the deposited coatings plotted in a ternary diagram. The coatings prepared at ambient temperature are depicted in black and the coatings prepared at the elevated temperature are depicted in red. The composition corresponding to the W_2BC stoichiometry is marked in blue as reference. The difference in the composition of the coatings deposited with the same sputtering powers and at different substrate temperatures was within the error of measurement. Therefore, the deposition temperature had minimal influence on the coating composition, and any potential differences between the coating prepared at ambient temperature and the one prepared at the elevated temperature are considered to be the effect of the microstructure changes only.

3.1 Structure and mechanical properties

The X-ray diffractograms of the coatings are shown in Figure 3. All the diffractograms exhibited one broad peak in the 2θ range of 37.9 – 39.4° with a full width at half maximum (FWHM) of 5.8 - 9.9°. The width of this peak indicated a nearly amorphous microstructure of the coatings with only short-range ordering or nanocrystallites with the size of a few

nanometres present [23, 24]. Due to the width of the peak it was impossible to unambiguously identify the possible crystalline phase or phases present in the coatings, as the main diffractions corresponding to W_2BC and tungsten carbides and borides lie in this range of 2θ angles. However, a qualitative assessment of the X-ray diffractograms is possible. The position and width of the peak varied slightly with the change of the coating composition. Coating 1 with the lowest content of W exhibited the largest FWHM. The FWHM of coating 2 was smaller. Coating 3 with the highest content of W showed the smallest FWHM. This trend was the same for the coatings prepared at the ambient temperature and the elevated temperature. Smaller FWHM of the diffraction peaks generally corresponds to the larger size of nanocrystallites and better crystallinity of a material [23]. Therefore, it can be suspected that the higher content of W and lower contents of B and C in the W-B-C coatings led to a better atomic ordering in the deposited coatings although the coatings were still not fully crystalline.

Figure 4 shows the change in the microstructure of the coatings with different composition prepared at the elevated temperature of 500 °C. The coatings varied slightly in thickness (1.75 - 2.25 μm), however this was only due to the change of the powers applied to the targets. Coating 1_500°C with the lowest content of W showed the most pronounced columnar structure with columns 50~100 nm thick spanning the whole thickness of the coating. Coating 2_500°C with a composition equivalent to W_2BC exhibited a fine feather-like microstructure. Coating 3_500°C with the highest content of W showed the most compact glassy microstructure. A progressive refinement of the structure was thus observed with the increasing content of tungsten. A similar refinement was also observed in the case of the coatings deposited at ambient temperature. This agrees well with the combined SRIM [25] and SIMTRA [26] simulations yielding that the energy influx to the growing coating increases with increasing W content [27]. Refinement of the coating structure with increasing energy flux is a well-documented phenomenon [28, 29]. Furthermore, tungsten as the heaviest

element exhibits the most efficient momentum transfer leading to densification of the coating microstructure [30, 31, 32].

The hardness of deposited coatings is shown in Figure 5a. The hardness of the coatings prepared at ambient temperature did not significantly change and was 22.7 ± 0.3 GPa. The hardness of the coatings deposited at elevated temperature was around 25.1 ± 0.9 GPa. Therefore, the hardness increased with the deposition temperature even though the XRD diffractograms did not reveal any significant structural changes in the coatings with temperature. The width of the peaks varied more with changes in composition, which is not reflected in changes in hardness. No direct correlation between XRD diffractograms and mechanical properties has been observed. The effective elastic modulus of the coatings is shown in Figure 5b. The effective elastic modulus of the coatings prepared at ambient temperature was similar for coatings 1_AT and 2_AT (~ 310 GPa) and a slight decrease in the effective elastic modulus of $\sim 10\%$ was observed for coating 3_AT with the highest tungsten content. The effective elastic modulus of the coatings 1_500°C and 3_500°C was constant within the margin of error (~ 315 GPa), while the effective elastic modulus for coating 2_500°C decreased by $\sim 15\%$ to 260 GPa.

Coating 3_500°C exhibited the highest hardness (26.2 GPa) and effective elastic modulus (320 GPa). The hardest coating exhibited the finest glassy microstructure as shown by the SEM micrograph of the cross section (Fig. 4c), as well as the lowest FWHM of the XRD diffraction peak indicating the highest degree of atom ordering in the studied coatings.

The ratio of the hardness to the effective elastic modulus H/E^* has been shown to point to the fracture toughness of a material, whereby a larger H/E^* ratio is correlated with the better fracture resistance of a material [33, 34]. The H/E^* ratio of the coatings is depicted in Figure 5c. The H/E^* ratio of the coatings prepared at ambient temperature was similar for 1_AT and 2_AT at the value of ~ 0.072 and it increased by $\sim 10\%$ to 0.08 for coating 3_AT with the

highest content of W. The H/E^* ratio was similar ~ 0.082 for coatings 1_500°C and 3_500°C and was $\sim 10\%$ higher (0.092) for coating 2_500°C indicating possibly better fracture resistance for this coating. The H/E^* ratio of the coatings prepared at an elevated temperature was always equal to or higher than that of the coatings prepared at an ambient temperature with corresponding composition.

The resistance to plastic deformation and wear behaviour of a material are often considered to depend on the H^3/E^{*2} ratio [34, 35]. The H^3/E^{*2} ratio is shown in Figure 5d. The evolution of the H^3/E^{*2} ratio shows the same trend as in the case of the H/E^* ratio, but more pronounced. This can be seen best in the comparison of the coatings with similar chemical composition deposited at different temperatures. A significant increase of the H^3/E^{*2} ratio by 30 ~ 65% was always observed with the higher deposition temperature, suggesting better tribological performance of the coatings prepared at the elevated temperature.

3.2 Tribological properties

The study of the tribological properties of the W-B-C coatings was the main focus of this work. The influence of the coating composition and deposition temperature on the wear behaviour of the coatings was investigated. The influence of the wear condition in terms of load and temperature was studied in detail.

3.2.1 Coefficient of friction

The CoF of the coatings was measured at 1 N load. As seen in Figure 6a, the coating 1_AT showed a low CoF with a short run-in period and strong fluctuations indicating delaminations of the coating in the wear track. The optical micrograph of the wear track of the coating 1_AT is shown in Figure 6b. The wear track showed severe delamination at the outer edge and a high amount of wear debris around the wear track. EDX measurements of the wear track have confirmed that the coating was fully delaminated at the outer edge of the wear track, where only

iron from the substrate was detected. It was also accompanied by severe abrasion of the counterpart ball as shown in Figure 6c.

In comparison, the CoF evolution of the coating 1_500°C in Figure 6d showed a higher CoF with a longer run in period, although the CoF curve was significantly smoother and exhibited much smaller fluctuations compared to coating 1_AT. The wear track was considerably narrower. No significant delamination and much less amount of wear debris was observed for coating 1_500°C, which can be seen in Figure 6e. The counterpart wear scar for coating 1_500°C shown in Figure 6f was also significantly smaller compared to coating 1_AT. All other tested coatings exhibited behaviour similar to coating 1_500°C with a smooth CoF evolution, small amount of wear debris and no significant delamination.

The mean CoF of the coatings is summarized in a ternary diagram in Figure 7, where the coatings deposited at ambient temperature are shown as black circles and the coatings produced at elevated temperature are depicted as red triangles. The CoF values ranged from 0.36 to 1.05 depending on the coating composition and the deposition temperature. The friction coefficient increased with increasing the content of W. This evolution of the CoF is in accordance with the CoFs of binary materials containing the mix of W and/or B and/or C reported in the literature that are plotted as blue squares at the edges of the ternary diagram in Fig. 7. Pure tungsten coatings exhibited a CoF of 0.85 [36]. Boron doped W coatings with 85.1% of tungsten had a CoF of 0.82 [20] and the WB coatings created through boronisation showed a CoF of 0.72 [37]. Tungsten carbide exhibits a high CoF of up to 0.95 [38]. On the other hand, B-C coatings showed a much lower CoF ranging from 0.15 [19] to 0.35 [39]. DLC coatings doped with tungsten exhibited a CoF ranging from 0.09 to 0.22, where coatings with a higher content of W (up to 25 at.%) exhibited a higher CoF [38]. A similar observation was also reported, where DLC coatings doped with W showed an increase in the CoF from 0.26 to 0.34 when the W content was increased from 0 to 27.7% [40]. Therefore, the ternary W-B-C diagram in Fig. 7 can be roughly split into 3 domains that are coloured in green, yellow and rose – the first one

including the coatings with tungsten content $\lesssim 30$ at.% that exhibit CoFs $\lesssim 0.25$, the second one with tungsten content $30 \sim 45$ at.% having CoFs of $0.25 \sim 0.8$ and the last domain of $\gtrsim 45$ at.% W coatings with CoF $\gtrsim 0.8$. The prepared W-B-C coatings 1_AT, 1_500°C, 2_AT and 2_500°C with stoichiometry closer to that of W_2BC fall into the medium range of CoFs, while coatings 3_AT and 3_500°C with higher amount of tungsten fall into the high CoF region.

The CoF of the W-B-C coatings was also influenced by the deposition temperature. A higher deposition temperature led to an increase in the CoF for coatings 1_AT and 1_500°C and a decrease in the friction coefficient for coatings 2_AT and 2_500°C. The measured CoF for coatings 3_AT and 3_500°C was not significantly affected by the deposition temperature.

3.2.2 Wear resistance

The wear rate of all the coatings tested at 1 N load is plotted in Figure 8. Only coatings 1_AT and 1_500°C exhibited the dependence of the wear rate on the deposition temperature. The wear rate of coating 1_AT was significantly higher than the wear rate of coating 1_500°C. The wear track of coating 1_AT exhibited delamination at the outer edge of the wear track as shown in Fig. 6a while no delamination was observed for coating 1_500°C in Fig. 6d. No dependence of wear on the deposition temperature was observed for coatings 2_AT, 2_500°C, 3_AT and 3_500°C, where coatings with identical composition exhibited similar wear and no delamination regardless of deposition temperature. Despite the fact that all of the coatings prepared at elevated temperature exhibited the H^3/E^{*2} ratio significantly higher than the corresponding coatings prepared at ambient temperature, the difference in wear observed for coating pairs 2 and 3 has been within the error rate of the measurement. Therefore, the H^3/E^{*2} ratio is not the only parameter defining the wear resistance of the coating, however the observed coating failure for coating 1_AT may also be caused by other effects that are not reflected by the H^3/E^{*2} ratio such as the adhesion failure of the coating.

3.2.3 Effect of tribotest temperature

Several coatings were selected for tribological testing at elevated temperature. The coatings were selected based on their wear behaviour at ambient temperature and under the load of 5N. Some coatings failed in these tests due to low adhesion and only the most resilient coatings were therefore tested at high temperatures to emulate real conditions during industrial applications such as dry machining. All surviving coatings were those prepared at elevated temperature, which agrees well with their higher H^3/E^2 ratio.

The dependence of the CoF on the test temperature for the coatings 2_500°C and 3_500°C is shown in Fig. 9. The CoF was stable until ~ 500 - 600°C and noticeably decreased as the test temperature was further increased. For most coatings, this decrease of the CoF was, however, accompanied by a severe increase in the wear rate of the coatings as shown in Fig. 9b. Coating 2_500°C shown in Fig. 9a exhibited an earlier wear increase which started at 300°C. The high wear rate was partly caused by delamination of the coatings from the substrate. This delamination was, however, not complete with parts of the coating in the wear track remaining intact. The increase in wear with temperature was not caused only by the changes in the coating properties. Other factors such as substrate softening probably played an important role in the coating delamination during the test as well. A comparison of the X-ray diffractograms of the coating 2_500°C as-deposited and after tribotested at 600°C in atmosphere is shown in Figure 10. The wide diffraction peak at $2\theta \sim 38^\circ$ disappeared after the high temperature tests under atmosphere and profound sharp diffraction peaks were present instead. The sharp peaks corresponded to WO_3 (blue), iron (black dashed) and iron oxides Fe_2O_3 (red dashed), Fe_3O_4 (grey dashed). The iron and iron oxides originated from the oxidation of the steel substrates and tungsten oxides originated from the oxidised tungsten from the coating. The presence of the WO_3 phase in the weartrack was clearly confirmed by XRD from a spot focused only in the weartrack as is shown in Figure 11. WO_3 belongs to the group of the so-called Magnéli phases. It was formed at high temperatures (550 - 700°C) and acted as a solid-state lubricant [14, 41]. As a consequence, a significant increase in wear was

attributed to the low hardness of the Magnéli phases. The formation of Magnéli phases has been observed for all tested coatings.

4 Conclusion

Three sets of W-B-C coatings were deposited using mid-frequency pulsed-DC magnetron sputtering in differing deposition conditions to study the effect of coating composition and the deposition parameters on the structure, mechanical and tribological properties of the coatings. X-ray diffractometry has shown one broad peak indicating a low level of crystallinity. The degree of atom ordering was mildly influenced by the coating composition, where a higher content of W resulted in a higher degree of atom ordering. The effect of the deposition temperature on the degree of atom ordering was negligible. The hardness of the coatings ranged from 21.5 to 26.2 GPa depending on the deposition conditions. The coatings prepared at 500 °C exhibited higher hardness compared to the coatings prepared at ambient temperature. The H^3/E^2 ratio was higher for the coatings prepared at the elevated temperature, pointing to better resistance to plastic deformation and better tribological performance. While the effect of H^3/E^2 ratio on the tribological properties was not clear from the measurements with 1 N load, it became apparent in 5 N load measurements. Only coatings with a high H^3/E^2 ratio did not fail in these tests.

The influence of the coating composition, deposition and testing conditions on the friction coefficient and wear rate was examined. The friction coefficient increased with increasing the content of W and decreasing the content of B for all the W-B-C coatings. This is in good agreement with available literature, where binary coatings containing tungsten exhibit a higher CoF with an increasing amount of tungsten. No clear influence of the deposition temperature on the friction coefficient was observed. The friction coefficient for all coatings decreased when the testing temperature reached 500 – 600°C during high temperature

measurements. XRD analyses after high temperature tests have shown that this was due to the formation of W-O Magnéli phases, which acted as a solid-state lubricant. The decrease in CoF was accompanied by a significant increase in wear caused by the low hardness of the Magnéli phases.

Acknowledgements

This research has been supported by the project LO1411 (NPU I) funded by Ministry of Education, Youth and Sports of Czech Republic, project CZ.1.05/2.1.00/03.0086 funded by the European Regional Development Fund and GACR project 15-17875S.

References

- [1] W. D. Münz, Titanium aluminum nitride films: A new alternative to TiN coatings, *Journal of Vacuum Science and Technology A: Vacuum, Surfaces, and Films* 4 (1986) 2717 - 2725.
- [2] O. Knotek, W. D. Münz, T. Leyendecker, Industrial deposition of binary, ternary, and quaternary nitrides of titanium, zirconium, and aluminum, *Journal of Vacuum Science and Technology A: Vacuum, Surfaces, and Films* 5 (1987) 2173 - 2179.
- [3] S. PalDey, S.C. Deevi, Single layer and multilayer wear resistant coatings of (Ti,Al)N: a review, In *Materials Science and Engineering: A* 342 (2003) 58-79, ISSN 0921-5093.
- [4] K. Chen, L. R. Zhao, J. Rodgers, J. S. Tse, Alloying effects on elastic properties of TiN-based nitrides, *Journal of Physics D: Applied Physics* 36 (2003) 2725-2729.
- [5] S. Vepřek, The search for novel, superhard materials, *Journal of Vacuum Science and Technology A: Vacuum, Surfaces, and Films* 17 (1999) 2401-2420.
- [6] H. Bolvardi, J. Emmerlich, M. to Baben, D. Music, J. von Appen, R. Dronskowski, J. M. Schneider, Systematic study on the electronic structure and mechanical properties of X_2BC ($X = Mo, Ti, V, Zr, Nb, Hf, Ta$ and W), *Journal of Physics: Condens. Matter* 25 (2013) 045501.
- [7] K. Chen, L. R. Zhao, J. Rodgers, J. S. Tse, Alloying effects on elastic properties of TiN-based nitrides, *Journal of Physics D.: Applied Physics* 36 (2003) 2725.
- [8] S. I. Wright, Estimation of single-crystal elastic constants from textured polycrystal measurements, *Journal of Applied Crystallography* 27 (1994) 794.
- [9] H. Yao, L. Ouyang, W-Y. Ching, Ab Initio Calculation of Elastic Constants of Ceramic Crystals, *Journal of the American Ceramic Society* 90 (2007) 3194.
- [10] J. Emmerlich, D. Music, M. Braun, P. Fayek, F. Munnik, J.M. Schneider, A proposal for an unusually stiff and moderately ductile hard coating material: Mo_2BC , *Journal of Physics D.: Applied Physics* 42 (2009) 185406.
- [11] H. Bolvardi, J. Emmerlich, S. Mráz, M. Arndt, H. Rudigier, J. M. Schneider, Low temperature synthesis of Mo_2BC thin films, *Thin Solid Films* 542 (2013) 5–7.
- [12] H. Bolvardi, D. Music, J. M. Schneider, Interaction of Al with O_2 exposed Mo_2BC , *Applied Surface Science* 332 (2015) 699–703.
- [13] S. Djaziri, S. Gleich, H. Bolvardi, C. Kirchlechner, M. Hans, C. Scheu, J.M. Schneider, G. Dehm, Are Mo_2BC nanocrystalline coatings damage resistant? Insights from comparative tension experiments, *Surface and Coatings Technology* 289 (2016) 213–218.
- [14] G. Gassner, P.H. Mayrhofer, K. Kutschej, C. Mitterer, M. Kathrein, Magnéli phase formation of PVD Mo-N and W-N coatings, *Surface and Coatings Technology* 201 (2006) 3335–3341.
- [15] Azushima, Y. Tanno, H. Iwata, K. Aoki, Coefficients of friction of TiN coatings with preferred grain orientations under dry condition, *Wear* 265 (2008) 1017–1022.
- [16] T. Polcar, T. Kubart, R. Novák, L. Kopecký, P. Šíroky, Comparison of tribological behaviour of TiN, TiCN and CrN at elevated temperatures, *Surface and Coatings Technology* 193 (2005) 192 – 199.
- [17] J.L. Mo, M.H. Zhu, B. Lei, Y.X. Leng, N. Huang, Comparison of tribological behaviours of AlCrN and TiAlN coatings—Deposited by physical vapor deposition, *Wear* 263 (2007) 1423–1429.

- [18] J. Hardell, B. Prakash, Tribological performance of surface engineered tool steel at elevated temperatures, *Int. Journal of Refractory Metals and Hard Materials* 28 (2010) 106–114.
- [19] J. K. Sonber, P. K. Limaye, T. S. R. Ch. Murthy, K. Sairam, A. Nagaraj, N. L. Soni, R. J. Patel, J.K. Chakravartty, Tribological properties of boron carbide in sliding against WC ball, *Int. Journal of Refractory Metals and Hard Materials* 51 (2015) 110–117.
- [20] L. Yang, K. Zhang, Y. Zeng, X. Wang, S. Du, Ch. Tao, P. Ren, X. Cui, M. Wen, Boron doped bcc-W films: Achieving excellent mechanical properties and tribological performance by regulating substrate bias voltage, *Applied Surface Science* 423 (2017) 275–282.
- [21] Y. T. Pei, C. Q. Chen, K. P. Shaha, J. Th. M. De Hosson, J. W. Bradley, S. A. Voronin, M. Čada, Microstructural control of TiC/a-C nanocomposite coatings with pulsed magnetron sputtering, *Acta Materialia* 56 (2008) 696-709.
- [22] W.C. Oliver, G.M. Pharr, Measurement of hardness and elastic modulus by instrumented indentation: advances in understanding and refinements to methodology, *Journal of Materials Research* 19 (2004) 3–20.
- [23] B. D. Cullity, *Elements of X-ray diffraction*, Addison-Wesley Publishing company (1956).
- [24] D. Galvan, Y. T. Pei, J.T.M. De Hosson, *Surface & Coatings Technology* 201 (2006) 590–598.
- [25] J. Ziegler, SRIM 2008, [software], <http://www.srim.org/>
- [26] K. Van Aeken, S. Mahieu, D. Depla, The metal flux from a rotating cylindrical magnetron: a Monte Carlo simulation, *Journal of Physics D.: Applied Physics* 41 (2008) 20530, DOI 10.1088/0022-3727/41/20/205307.
- [27] M. Alishahi, S. Mirzaei, P. Souček, L. Zábranský, V. Buršíková, M. Stupavská, V. Peřina, K. Balázsi, Z. Czigány, P. Vašina, Evolution of structure and mechanical properties of hard yet fracture resistant WBC coatings with varying C/W ratio, *Surface and Coatings Technology* 340 (2018) 103-111. ISSN 0257-8972.
- [28] J. A. Thornton, Influence of apparatus geometry and deposition conditions on the structure and topography of thick sputtered coatings, *Journal of Vacuum Science and Technology* 11 (1974) 666 - 670.
- [29] Anders, A structure zone diagram including plasma-based deposition and ion etching, *Thin Solid Films* 518 (2010) 4087–4090.
- [30] G. Abadias, L.E. Koutsokeras, P. Guerin, P. Patsalas, Stress evolution in magnetron sputtered Ti–Zr–N and Ti–Ta–N films studied by in situ wafer curvature: Role of energetic particles, *Thin Solid Films* 518 (2009) 1532-1537.
- [31] H. Windischmann, Intrinsic stress in sputter-deposited thin films, *Critical Reviews in Solid State and Materials Science* 17 (1992) 547-596.
- [32] G. Greczynski, J. Lu, J. Jensen, I. Petrov, J.E. Greene, S. Bolz, W. Kölker, C. Schiffrers, O. Lemmer, L. Hultman, Strain-free, single-phase metastable Ti_{0.38}Al_{0.62}N alloys with high hardness: metal-ion energy vs. momentum effects during film growth by hybrid high-power pulsed/dc magnetron cosputtering, *Thin Solid Films* 556 (2014) 87-98.
- [33] Leyland, A. Matthews, On the significance of the H/E ratio in wear control: a nano-composite coating approach to optimised tribological behaviour, *Wear* 246 (2000) 1–11.

- [34] J. Musil, F. Kunc, H. Zeman, H. Polakova, Relationships between hardness, Young's modulus and elastic recovery in hard nanocomposite coatings, *Surface and Coatings Technology* 154 (2002) 304–313.
- [35] Y.T. Pei, D. Galvan, J.T.M. De Hosson, A. Cavaleiro, Nanostructured TiC/a-C coatings for low friction and wear resistant applications, *Surface and Coatings Technology* 198 (2005) 44–50.
- [36] W. G. Sawyer, T. A. Blanchet, Lubrication of Mo, W, and their Alloys with H₂S gas admixtures to room temperature air, *Wear* 225–229 (1999) 581–586.
- [37] M. Usta, I. Ozbek, C. Bindal, A. H. Ucisik, S. Ingole, H. Liang, A comparative study of borided pure niobium, tungsten and chromium, *Vacuum* 80 (2006) 1321–1325.
- [38] W. H. Kao, Optimized a-C:W_x% coatings with enhanced tribological properties and improved micro-drilling performance, *Surface and Coatings Technology* 201 (2007) 7392–7400.
- [39] S. Liza, N. Ohtake, H. Akasaka, J. M. Munoz- Guijosa, Tribological and thermal stability study of nanoporous amorphous boron carbide films prepared by pulsed plasma chemical vapor deposition, *Science and Technology of Advanced Materials* 16 (2015) 035007.
- [40] W. Yue, S. Wang, Z. Fu, X. Gao, X. Yu, J. Liu, Influence of W content on microstructural, mechanical and tribological properties of sulfurized W-doped diamond-like carbon coatings, *Surface and Coatings Technology* 218 (2013) 47–56.
- [41] E. Lugscheider, S. Bärwulf, C. Barimani, Properties of tungsten and vanadium oxides deposited by MSIP-PVD process for self-lubricating applications, *Surface and Coatings Technology* 120–121 (1999) 458–464.

Table I: Deposition conditions of prepared coatings and measurements results, EDX composition, XRD peak position and width, hardness, effective elastic modulus and friction coefficient for 1 N load measurements.

Coating No.	Power to target (W)			T _{dep} (°C)	W (at. %)	B (at. %)	C (at. %)	2θ [°]	FWHM [°]	H [GPa]	E* [GPa]	μ at 1N load
	W	B ₄ C	graphite									
1_AT	70	150	100	AT	40	32	28	38.2	9.3	22.7 ± 0.4	310 ± 9	0.36 ± 0.04
1_500°C	70	150	100	500	39	32	29	38.5	9.9	25.2 ± 0.7	310 ± 6	0.61 ± 0.05
2_AT	70	102	200	AT	48	26	26	38.3	8.3	22.8 ± 0.8	310 ± 8	0.92 ± 0.05
2_500°C	70	102	200	500	44	28	28	38.3	7.5	23.9 ± 1.8	260 ± 17	0.77 ± 0.03
3_AT	120	102	200	AT	65	15	20	39.1	5.8	22.6 ± 0.3	290 ± 9	0.97 ± 0.04
3_500°C	120	102	200	500	67	13	20	39.4	5.9	26.2 ± 2.0	320 ± 16	1.00 ± 0.04

Figures

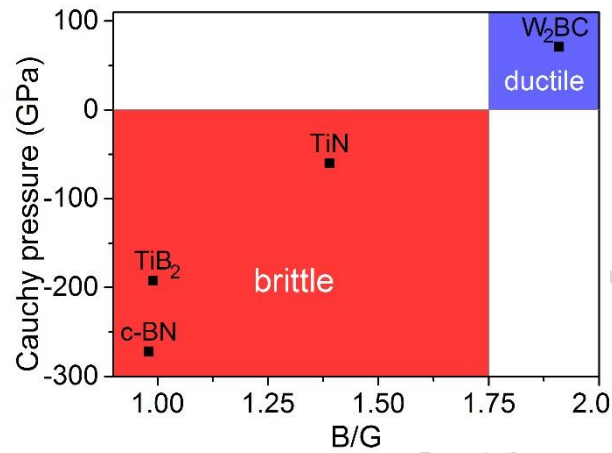


Figure 1 Cauchy pressure and the B/G ratio of commonly used protective coatings as well as the values calculated for W₂BC [6, 7, 8, 9]. While the standard protective coatings fall into the category of brittle materials (indicated in red), W₂BC lies in the ductile region (indicated in blue).

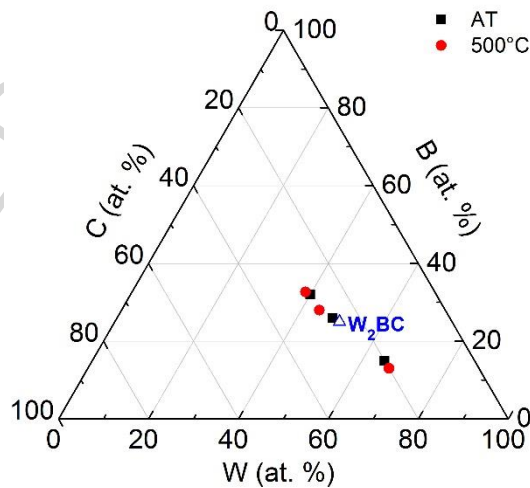


Figure 2 Composition of prepared coatings measured by EDX in reference to the stoichiometric W₂BC.

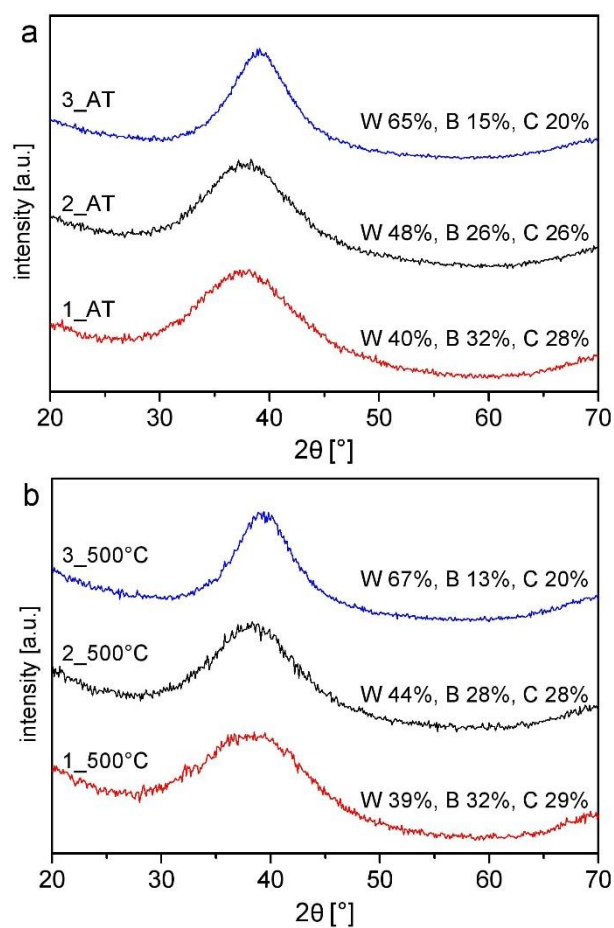


Figure 3 X-ray diffractogram of coatings prepared at ambient temperature (a) and 500°C (b).

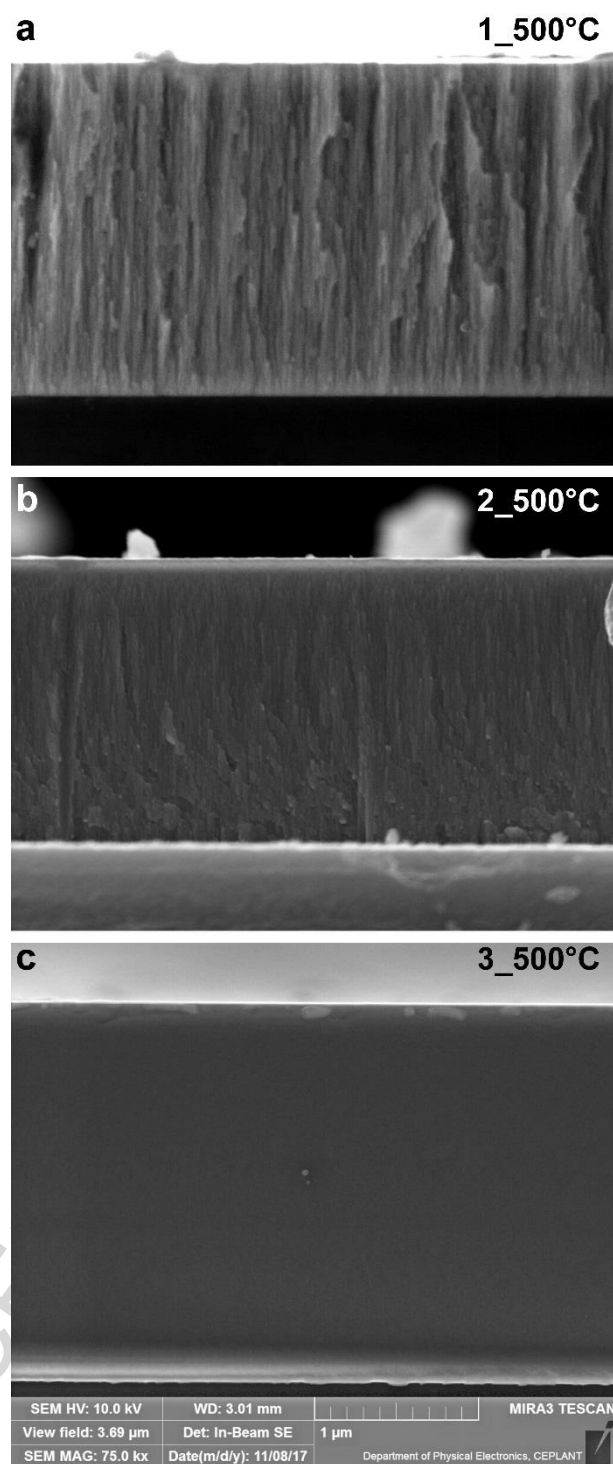


Figure 4 Cross sectional SEM micrograph showing the microstructure evolution versus composition of the coatings: (a) 1_500°C, (b) 2_500°C, and (c) 3_500°C.

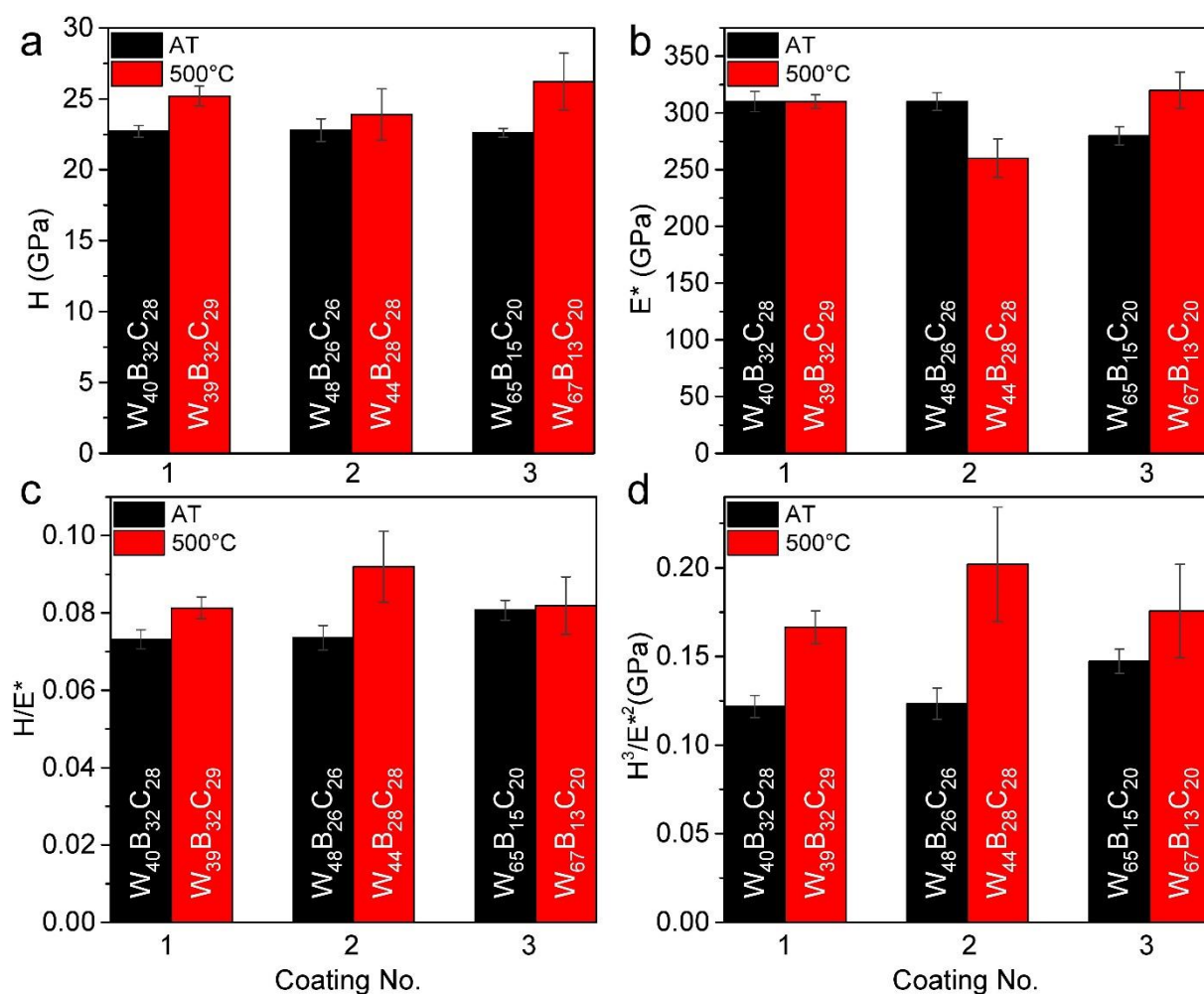


Figure 5 Comparison of the measured mechanical properties of the coatings depending on the composition and deposition temperature: (a) hardness H, (b) effective elastic modulus E*, (c) H/E* ratio, and (d) H³/E*² ratio.

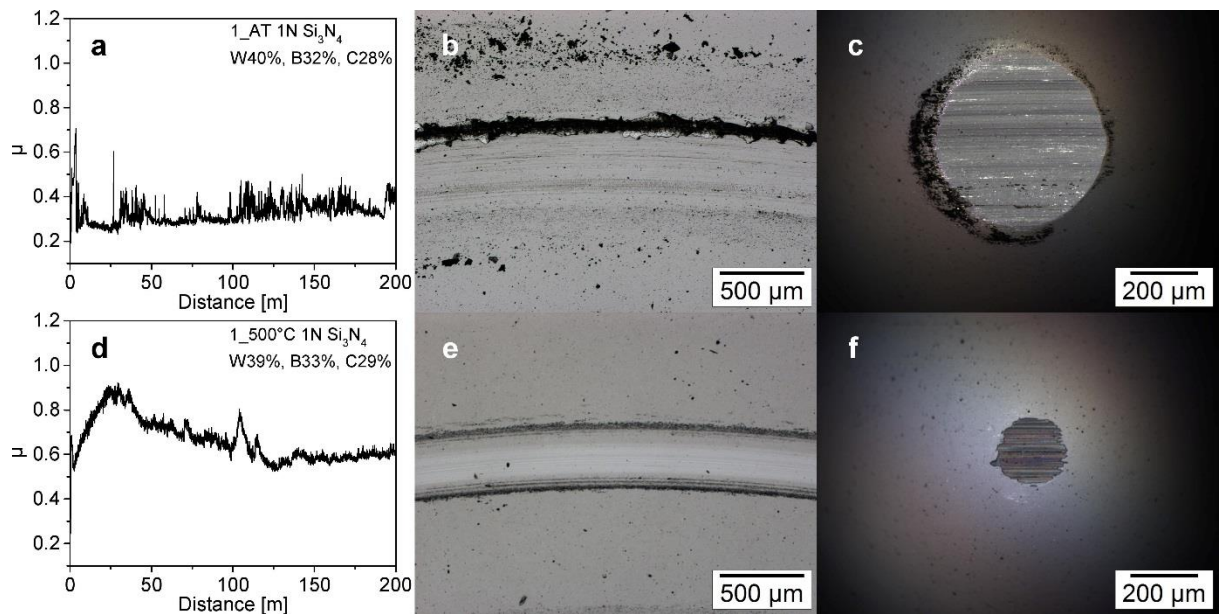


Figure 6 Coefficient of friction (μ), optical images of wear track and wear scar of the counterpart ball for coating 1_AT (a, b, c) and 1_500°C (d, e, f). The tests were conducted at 1 N load.

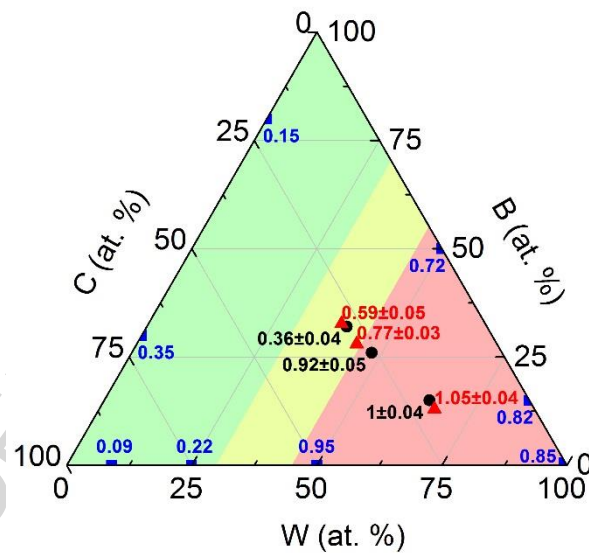


Figure 7 Measured friction coefficient of the coatings prepared at ambient temperature (black circles) and elevated temperature (red triangles) compared to the friction coefficient of binary coatings found in literature (blue squares) [19, 20, 36, 37, 38, 39].

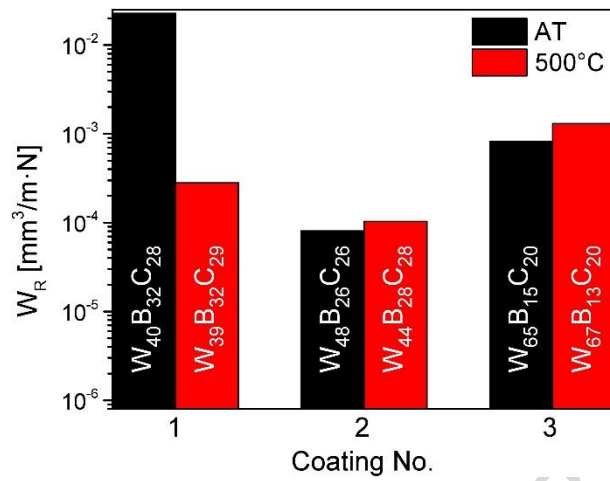


Figure 8 Influence of composition and deposition temperature on the wear rate of the coatings tested at 1 N load.

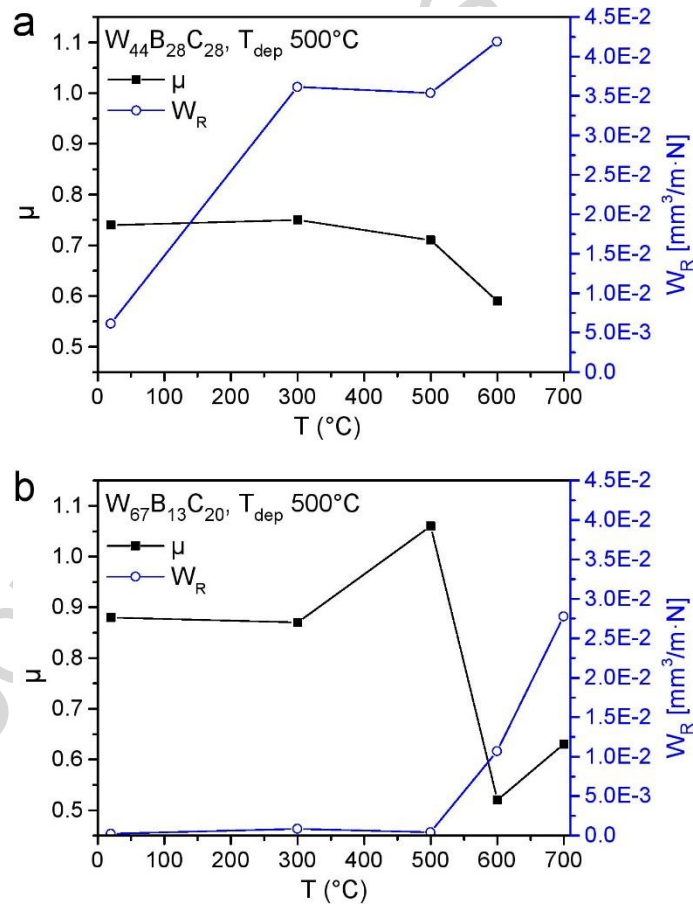


Figure 9 Effect of test temperature on the friction coefficient and wear rate: (a) coating 2_500°C and (b) coating 3_500°C tested under 5 N normal load.

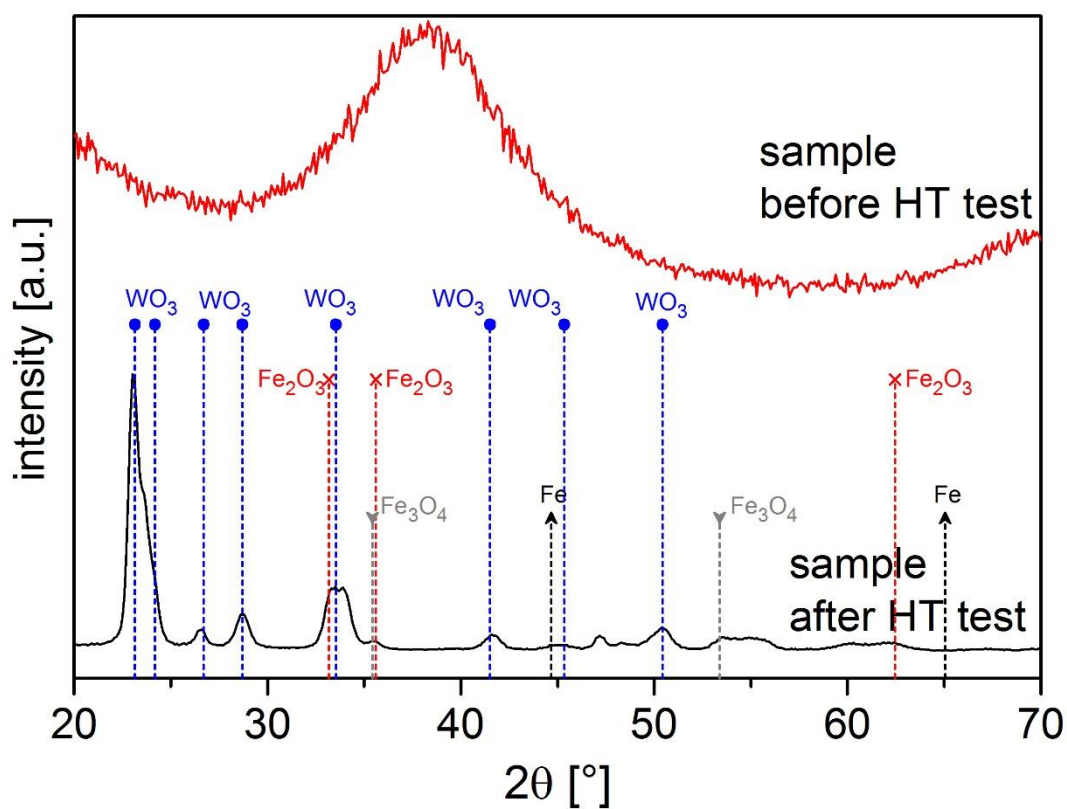


Figure 10 X-ray diffractogram of the surface of coating 2_500°C before and after high temperature measurements. After the high temperature measurement, the formation of WO_3 (blue) was observed, as well as iron (black) and iron oxides Fe_2O_3 (red), Fe_3O_4 (grey).

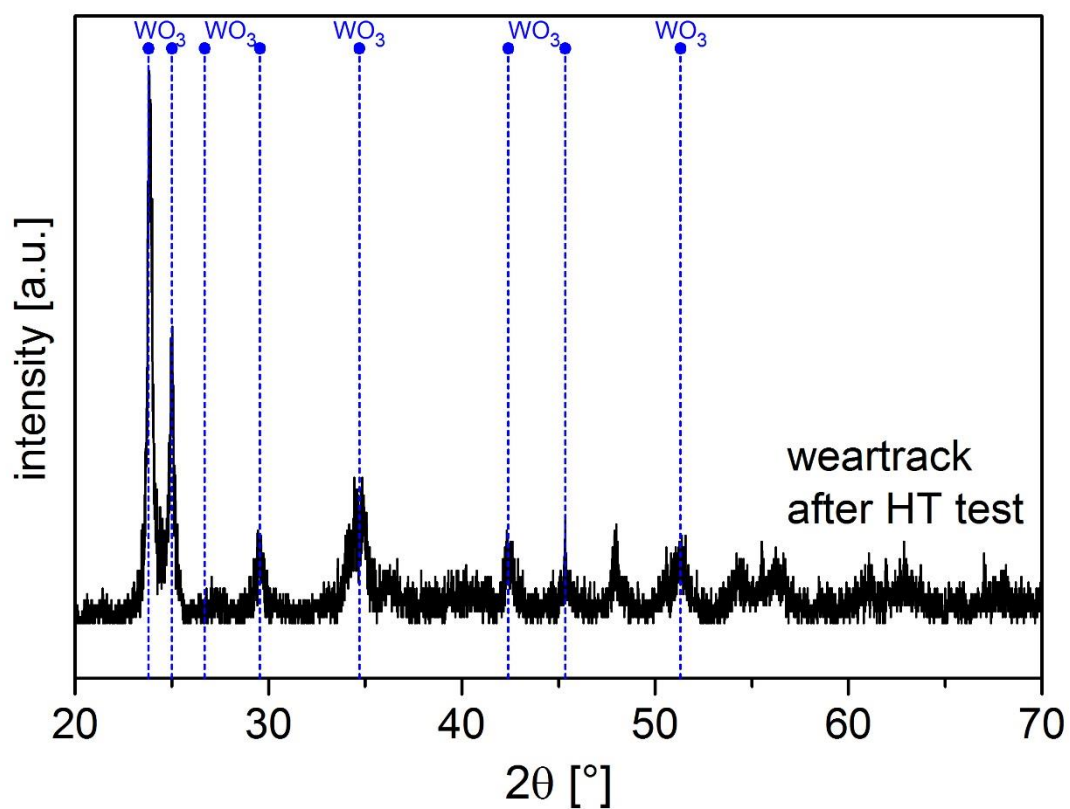


Figure 11 X-ray diffractogram of the weartrack of coating 2_500°C after the measurement at 600°C. The formation of WO₃ was observed in the weartrack.

Highlights

- Amorphous and nanocrystalline coatings were prepared by p-DC magnetron sputtering
- Coatings prepared at elevated temperature exhibited higher hardness
- The amount of W was the main parameter influencing the friction coefficient
- Magnéli phases acting as solid-state lubricants were formed at high temperatures